ELSEVIER

Chemical Engineering Journal 88 (2002) 127–139

Chemical Engineering Journal

www.elsevier.com/locate/cej

Interdrop coalescence with mass transfer: comparison of the approximate drainage models with numerical results

A. Saboni [a,*], S. Alexandrova [a], C. Gourdon [b], A.K. Chesters [c]

[a] *Groupe Ecoulements, Transferts de Matière et de Chaleur, LTP, Dépt GTE, IUT, Universite de Caen, 120 rue de l'exode, 50000 Saint lô, France*
[b] *Laboratoire de Génie Chimique, URA CNRS 192, Ecole Nationale Supérieure d'Ingénieurs de Génie Chimique, Chemin de la loge, 31078 Toulouse Cedex, France*
[c] *Laboratory of Fluid Dynamics and Heat Transfer, Eindhoven University of Technology, P.O. Box 513, Eindhoven, The Netherlands*

Received 23 September 2001; received in revised form 5 November 2001; accepted 12 November 2001

Abstract

The partially mobile, plane-film model developed to describe film drainage and rupture during coalescence in liquid–liquid dispersions is extended to take account of interfacial-tension gradients generated by mass transfer. The resulting Marangoni forces are predicted to greatly accelerate film drainage (which in general corresponds to dispersed to continuous phase transfer) and to diminish film drainage in the negative case. The first model is based on the approximation of constant pressure and interfacial tensions outside the film. The predictions from this model agrees with observations and available numerical data, in the case of mass transfer from dispersed to continuous phase. While for mass transfer from continuous to dispersed phase, a second model is proposed, in this case the first model is adapted to take account of the location of the region of maximum concentration gradients, which moves radially outwards as a result of the growth of the continuous phase-concentration boundary layers. At large times, the new model predicts an asymptotic return to the drainage rate in the absence of mass transfer.

Keywords: Liquid–liquid; Film drainage; Coalescence; Mass transfer; Modeling

1. Introduction

While both the nature and the mechanism of the influence of mass transfer on drop coalescence in liquid–liquid dispersions are accepted (see e.g. Kleczek et al. [1], Gourdon and Casamatta [2]), except Saboni et al. [3], no quantitative models—even approximate ones—appear to have been developed. This is perhaps not surprising if one recalls that the requisite models in the absence of mass transfer are relatively recent.

For pure systems, numerical studies of the coupled processes of drop deformation and film drainage under the action of a constant interaction force have been carried out by Yiantsios and Davis [4] in the limits of immobile and partially mobile interfaces. The term partial mobility is used to indicate that drainage is controlled by the motion of the interfaces (this motion in turn being limited by viscous forces exerted by the drop phase), the contribution of the Poiseuille flow with respect to the interfaces being negligible. This is the most important regime from a practical point of view, full mobility or immobility arising only for extreme viscosity ratios (Abid and Chesters [5]). The additional influence of van der Waals forces, leading to film rupture in finite drainage time has been studied numerically in the immobile case (Yiantsios and Davis [6]) and in the partially mobile case (Saboni et al. [7]). The case of constant approach velocity of the drops has also been studied in the partially mobile case, with and without van der Waals forces (Abid and Chesters [5]).

In the presence of mass transfer, a numerical model of the drainage of liquid films between drops undergoing a constant interaction force has been developed (Saboni et al. [3]). The mathematical problem consisting of the coupled equations of flow and diffusion in each phase, subject to the boundary conditions at the interface, together with those provided by the interaction characteristics of the drops. The situation considered is that of partially mobile drainage, under the action of a constant force and in the absence of van der Waals forces. Numerical solutions were obtained for both positive and negative values of Marangoni parameter (corresponding to solute transfer both to and from the drops) for fixed, physically pertinent values of the other parameters, including

* Corresponding author. Tel.: +33-2-33-77-11-72; fax: +33-2-33-77-11-78.
E-mail addresses: asaboni@aol.com, ltp@stlo.unicaen.fr (A. Saboni).

1385-8947/02/$ – see front matter
PII: S1385-8947(01)00296-0

Nomenclature

a	film radius
a'	a/R_{eq}
A	Hamaker constant
c	parameter defined by Eq. (5)
C	solute concentration (mass fraction)
C_0	C-value adjacent to interface
ΔC^*	driving concentration difference for mass transfer
D	molecular diffusivity
D'	modified diffusion coefficient
f	acceleration/deceleration factor
F	interaction force exerted by one drop on another
F_{num}	numerically instantaneous acceleration/deceleration factors
F_1, F_2	instantaneous acceleration/deceleration factors predicted by models I and II
F_σ, F_p, F_w	force per unit volume of film due, respectively, to gradients of interfacial tension, gradients of pressure and van der Waals forces
h	film thickness
h_c	critical film-rupture thickness
h_{cen}	thickness at film center
h_{flat}	film thickness at which the drops become flattened
h_M	film thickness corresponding to Marangoni-accelerated rupture
h_{min}	minimum film thickness
h_0	initial film thickness
h_δ	film thickness, 2δ, at location where concentration boundary layers meet
H_c	dimensionless rupture thickness
k_1–k_3	constants of order unity
K	partition coefficient $dC_{d,0}/dC_0$
m	mass flux through the interface
Ma	Marangoni number
p	film pressure
P	transformed partition coefficient
Pe	Peclet number
r	radial coordinate
r_{dcmax}	r-value corresponding to maximum of $\partial C_0/\partial r$
r_{hmin}	r-value corresponding to h_{min}
R	drop radius
R_{eq}	equivalent radius, $2/(R_1^{-1} + R_2^{-1})$
S	area of the material element of the interface
t	time
t_c	time to drain to critical film-rupture thickness, h_c
t_i	interaction time of colliding drops
T	dilation time scale
u	radial velocity of the draining film
U	interface velocity
V	approach velocity of undeformed portions of drops
z	axial coordinate; distance perpendicular to interface
Z	dimensionless group determining the deceleration factor

Greek letters

δ	concentration boundary layer thickness
μ	dynamic viscosity
ρ	density
σ	interfacial tension
σ_{eff}	effective interfacial tension
$\Delta\sigma$	σ difference between film and outer region
τ	shear stress exerted on the interface
Σ	film tension

Subscripts

d	pertaining to the dispersed phase
0	in the absence of mass transfer
∞	in the bulk phase far from the interface

Superscript

*	transformed variable, as defined in the text

a large Peclet number for which the diffusion boundary layer within the drop is thin, thereby somewhat simplifying the equations to be solved.

Mass transfer from the dispersed to the continuous phase has been found to accelerate the process of film drainage and hence to increase the probability of coalescence during drop collisions. Mass transfer in the reverse direction retards drainage and reduces the coalescence probability. The effect of interphase mass transfer on film drainage arises from the extra ("Marangoni") forces generated by gradients of interfacial tension, associated with variations of the solute concentration over the interface. Thus, if transfer is from dispersed to continuous phase the thin film separating the drops rapidly comes to equilibrium with the high solute concentration in the drop while the interface outside the film takes on a concentration value intermediate between that in the drop and in the continuous phase. If, as usually is the case, the interfacial tension is a decreasing function of the interfacial concentration, the interfacial tension in the film will be lower than that outside the film. The resulting gradient of interfacial tension produces a tangential force on the interface which accelerates the radial motion of the film and so reduces the drainage time. If the mass transfer is in the opposite direction, the interfacial concentration in the film will be very low and the effect will be reversed.

While the numerical results are encouraging vis a vis the modeling of coalescence processes in systems undergoing

mass transfer, it should be emphasized that the developed theoretical and computational framework concerns solutes exhibiting no surface activity. In practice, one of the two phases is almost always aqueous and most solutes with sufficient affinity to be appreciably soluble in both phases (alcohols, organic acids, etc.) are amphipathic to a greater or lesser extent. The resulting surface activity leads to additional Marangoni effects which always retard drainage. The net effect of $D \rightarrow C$ transfer could then be either coalescence promotion or reduction, depending on the degree of surface activity of the transferring solute. While the incorporation of surface activity in the governing equations is relatively simple, it introduces at least one further dimensionless parameter. If the simulation of film rupture is included—as ultimately it must be—the number of computations required to explore this six-dimensional parameter-space is clearly prohibitively great. Two options then remain if coalescence is to be modeled as a local process within an overall simulation of the two phase flow concerned:

(a) Compute the drainage time, and thence the coalescence probabilities, at each point in the system as function of local conditions.
(b) Develop approximate models for the drainage time as a function of the parameters concerned and then use the simulations as "numerical experiments" to test and refine these models.

At the present time, option (a) is completely excluded by limitations in computational power. An example of option (b) in the four-parameter case is the aim of this paper.

2. Approximate drainage models

We consider two drops of the same Newtonian fluid suspended in another Newtonian fluid, which approach each other along the line of their centers at a constant force. Various regimes of drainage may be distinguished depending on the rigidity and mobility of the interface [8]. Here we consider only the drainage between deformable partially mobile interfaces. We consider also that the deformable part of the drop is very small in comparison with the drop radius. This is not as restrictive as it appears since only for gentle collisions is drainage typically rapid enough for coalescence to occur. So the partially mobile, plane-film model [8] developed to describe film drainage and rupture during coalescence in liquid–liquid dispersions, is extended to take account of interfacial-tension gradients generated by mass transfer.

2.1. In the absence of mass transfer

In the absence of mass transfer (pure liquid–liquid systems), Chesters [8] introduced a parallel-film model (Fig. 1)

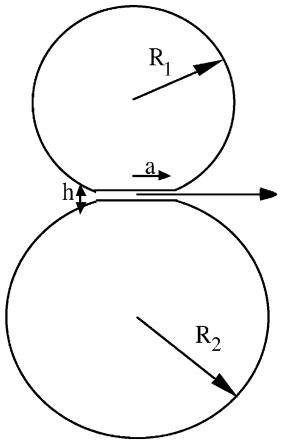

Fig. 1. Notation for plane parallel-film models.

describing drainage between colliding drops. The obtained expression is

$$\frac{2\mu_{\mathrm{d}} r k_1}{a h^2}\left(-\frac{\mathrm{d}h}{\mathrm{d}t}\right) = F_p = -\frac{\partial p}{\partial r} \tag{1}$$

where h is the film thickness, $\mathrm{d}h/\mathrm{d}t$ the thinning rate, μ_{d} the drop viscosity, r the radial coordinate, p the pressure, F_p the radial pressure force per unit film volume, k_1 the constant of order unity and a is a measure of the film radius related to the interaction force by

$$F = \int_0^{\text{large } r} 2\pi p r \,\mathrm{d}r = \pi a^2 \frac{2\sigma_0}{R_{\mathrm{eq}}} \tag{2}$$

where σ_0 is a characteristic value of the interfacial tension and the equivalent radius, R_{eq}, is defined by

$$\frac{2}{R_{\mathrm{eq}}} = \frac{1}{R_1} + \frac{1}{R_2} \tag{3}$$

where R_1 and R_2 are the radii of the two drops.

2.2. In the presence of mass transfer

2.2.1. The variation of interfacial concentration

Once the film thickness is well below h_δ, the film concentration will tend towards equilibrium with the drop, i.e. $C_{\mathrm{d},0}$ will tend towards $C_{\mathrm{d},\infty}$ so that

$$C_0 = \frac{C_{\mathrm{d},\infty}}{K} \tag{4}$$

Outside the film, however, C_0 will still be given by (Appendices A and B):

$$C_0 + c = \frac{C_\infty + c + PC_{\mathrm{d},\infty}/K}{1+P} \tag{5}$$

where P is the transformed partition parameter given by (B.9)

Thus interfacial concentration variation from the inside to the outside of the film is:

$$\Delta C_0^* = (C_0^*)_{\mathrm{ext}} - (C_0^*)_{\mathrm{film}} = \frac{C_\infty^* - C_{\mathrm{d},\infty}^*}{1+P} = -\frac{\Delta C^*}{1+P} \tag{6}$$

where C^*, C_d^* and ΔC^* are defined as

$$C^* = C, \qquad C_d^* = \frac{C_d}{K}, \qquad \Delta C^* = C_{d,\infty}^* - C_\infty^* \tag{7}$$

2.2.2. Model I

In the presence of mass transfer, the variation of species concentration over the interface engenders a corresponding variation in the interfacial tension. The variation of the interfacial tension produces a net tangential force per unit area, τ_σ

$$\tau_\sigma = \text{grad}\,\sigma \tag{8}$$

The radial force per unit volume of the film is consequently

$$F_\sigma = \frac{2\,\text{grad}\,\sigma}{h} \sim \frac{2\Delta\sigma}{ah} \sim \frac{2\Delta C_0^*}{ah}\frac{d\sigma}{dC_0^*} \sim -\frac{2\Delta C^*}{ah(1+P)}\frac{d\sigma}{dC_0} \tag{9}$$

where

$$\Delta\sigma = -\frac{\Delta C^*}{1+P}\frac{d\sigma}{dC_0} \tag{10}$$

F_σ must be included on the force balance

$$\frac{2\mu_d r k_1}{ah^2}\left(-\frac{dh}{dt}\right) = F_p + F_\sigma = -\frac{\partial p}{\partial r} + \frac{2}{h}\frac{\partial\sigma}{\partial r} \sim \frac{\Delta p}{a} + \frac{2}{h}\frac{\Delta\sigma}{a} \sim \frac{2\sigma}{R_{eq}} + \frac{2}{h}\frac{\Delta\sigma}{a} \tag{11}$$

which integrate with respect to r (limits of integration are 0 and a) to give (model I):

$$\frac{k_1\mu_d a}{h^2}\left(-\frac{dh}{dt}\right) \sim \frac{2\sigma}{R_{eq}} + \frac{2\Delta\sigma}{h} \tag{12}$$

Marangoni drainage is seen to dominate (i.e. $F_\sigma > F_p$) if $h < h_M$, where

$$h_M = -\frac{R_{eq}\Delta C^*}{1+P}\frac{1}{\sigma}\frac{d\sigma}{dC_0} \quad \text{or} \quad h_M = R_{eq}\left(\frac{\Delta\sigma}{\sigma}\right) \tag{13}$$

indicating that extremely small variations in interfacial tension are sufficient for Marangoni effect to dominate in the final stages of drainage.

2.2.3. Model II: modified film drainage

The plane film for coalescence under a constant force in the presence of mass transfer (model I) is based on the approximation of constant pressure and interfacial tension in the region outside the film. In reality, the region in which σ changes from a value corresponding to approximate equilibrium between film and drop to an approximately constant external value will be that in which the two continuous phase-concentration boundary layers meet. Since the thickness of these layers grows with time, this region will tend to move outside the film, where $h > h_{min}$ and the term $\Delta\sigma/h_{min}$ will then overestimate the influence of the mass transfer. This effect offers a possible explanation of the fact that the model I predicts complete blockage of coalescence by moderate levels of mass transfer from continuous to dispersed phase, whereas both experiment and numerical simulation indicate merely a moderate increase in the drainage times.

The modified film drainage law is once more obtained by integrating the force balance on a film element with respect to r

$$\frac{k_1\mu_d a}{h^2}\left(-\frac{dh}{dt}\right) \sim \frac{2\sigma}{R_{eq}} + \frac{2\Delta\sigma}{h_\delta} \tag{14}$$

The Marangoni term $2/h\,(\partial\sigma/\partial r)$, however, is now supposed significant only in a narrow range of r-values in the regions where $h = h_\delta$ and its integral is thus given by $2\Delta\sigma/h_\delta$ (h_δ is given in Appendix D), yielding

$$\frac{k_1\mu_d a}{h^2}\left(-\frac{dh}{dt}\right) \sim \frac{2\sigma}{R_{eq}} + \frac{2\Delta\sigma}{k_2(Dt)^{1/2}} \tag{15}$$

where k_2 is a constant in the order of 1. In contrast with (12), the Marangoni term in (15) becomes weaker as time progress, drainage tending asymptotically to the rate in the absence of mass transfer.

Now integrating with respect to t, (15) yields

$$k_1\mu_d a\left(\frac{1}{h} - \frac{1}{h_0}\right) = \frac{2\sigma}{R_{eq}}t + \frac{2\Delta\sigma}{k_2}\left(\frac{t}{D}\right)^{1/2} \tag{16a}$$

or

$$\frac{k_1\mu_d a}{h} = \frac{2\sigma}{R_{eq}}t + \frac{2\Delta\sigma}{k_2}\left(\frac{t}{D}\right)^{1/2} \tag{16b}$$

provided tha $h \ll h_0$.

3. Comparison of drainage models I and II with numerical results

3.1. Numerical approach

Details of the theory involved in the calculation of the drainage of partially mobile liquid films between drops undergoing a constant interaction force in the presence of mass transfer are given by Saboni et al. [3]. A brief summary is given in this paper. The mathematical problem consisting of the coupled equations of flow and diffusion in each phase, subject to the boundary conditions at the interface, together with those provided by the interaction characteristics of the drops. Numerical solutions were obtained for both positive and negative values of Marangoni parameter (corresponding to solute transfer both to and from the drops).

Expressed in terms of transformed variables

$$r^* = \frac{r}{R_{eq}a'}, \qquad h^* = \frac{h}{R_{eq}a'^2}, \qquad t^* = \left(\frac{a'\sigma}{R_{eq}\mu_d}\right)t,$$

$$a' = \frac{a}{R_{eq}}$$

the equations governing drainage containing four dimensionless parameters given as

$$Ma = \frac{\Delta C^*}{a'^2}\frac{1}{\sigma}\frac{\mathrm{d}\sigma}{\mathrm{d}C_0}, \qquad Pe = \frac{(a')^5 R_{\mathrm{eq}}\sigma_0}{\mu_{\mathrm{d}} D},$$

$$Pe_{\mathrm{d}} = \frac{(a')^3 R_{\mathrm{eq}}\sigma_0}{\mu_{\mathrm{d}} D_{\mathrm{d}}}, \qquad P = K\frac{\rho_{\mathrm{d}} D'_{\mathrm{d}}\sqrt{D}}{\rho D'\sqrt{D_{\mathrm{d}}}}$$

Ma represents the influence of Marangoni forces, *Pe* a weighted Peclet number for the continuous phase based on R_{eq} and the characteristic velocity, σ/μ, and weighted by the factor $(a')^5$. Pe_{d} represents a Peclet number for the dispersed phase, it governs the relative importance of diffusion and convection and in particular the relative thickness of the concentration boundary layer. *P*, governs the interfacial concentration in the external region.

The starting point for the computation is taken as the maximum value of *Pe* consistent with the requirement of a' to be small, corresponding to $a' = 0.1$, $R = 1\,\mathrm{mm}$, $\sigma_0 = 2.5 \times 10^{-2}\,\mathrm{N/m}$, $\mu_{\mathrm{d}} = 10^{-3}\,\mathrm{Pa\,s}$, $D = 10^{-9}\,\mathrm{m^2/s}$, yielding $Pe = 250$. In the simplest case, in which $\rho_{\mathrm{d}} = \rho$, $D_{\mathrm{d}} = D$, and $K = 1$, this situation then yields $Pe_{\mathrm{d}} = 2.5 \times 10^4$ and $P = 1$. Since $-(1/\sigma)(\mathrm{d}\sigma/\mathrm{d}C)$ is of order 1, the value of *Ma* explored in the present simulations (once more $a' = 0.1$) correspond to $Ma = -100\Delta C^*$.

In the absence of mass transfer, Fig. 2 shows the process of film formation which involves flattening followed by the development of dimples. In the presence of mass transfer, the effects are illustrated in Figs. 3 and 4, which may be compared with the neutral case (Fig. 2). The resulting drainage rates, in the presence of mass transfer, are shown in Figs. 5 and 6, together with the neutral case and other parameters combination. In the studied cases flattening precedes the onset of Marangoni effects, the thickness of the continuous phase-concentration boundary layers still being less than the film thickness at this point. Thereafter, the boundary layers meet in the region of minimum film thickness. The result is an acceleration of the local drainage rate in the case of negative Marangoni numbers, leading to an intensification of the dimple (Figs. 3 and 5), while for positive *Ma*-values liquid is pulled into this region suppressing dimple development (Figs. 4 and 6). For the larger negative Marangoni number ($Ma = -1$), final drainage rates are two orders of magnitude higher than for the same film thickness in the neutral case, while for $Ma = +1$ drainage is completely arrested. Assuming as discussed in the preceding paragraph, that *Ma* is of order of $100\Delta C^*$, this dramatic Marangoni effect occurs at concentrations differences of a few percent.

The picture provided by the computations is consistent both with the pulsed column experiments discussed in Section 1 and with the experiments of Kourio and co-workers [9,10]. The mass transfer $D \rightarrow C$ strongly promotes coalescence and $C \rightarrow D$ transfer reduces it. The latter effect was found by Kourio to be relatively weak, however, drainage times for $C \rightarrow D$ transfer are greater, but of the same order, as those in the absence of mass transfer. Additional computations, using other values of the four parameters, suggest that the arrest of drainage in the present case is only temporary (at higher time the equilibrium between the two phases is reached), final drainage rates being close to those in the absence of mass transfer. As the overall drainage time is dominated by the final stages in many cases, this time is only mildly increased

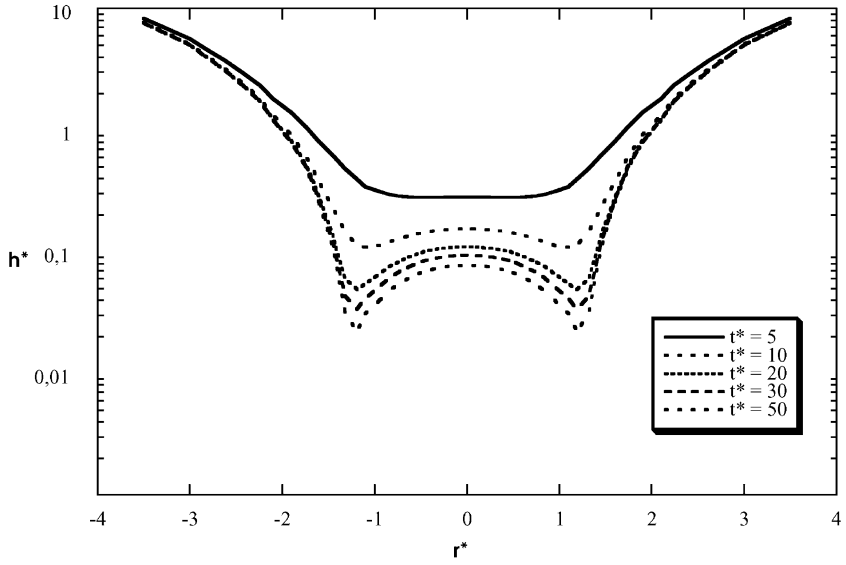

Fig. 2. Dimensionless film thickness, h^*, as a function of dimensionless radial position, r^*, and dimensionless time, t^*, in the absence of van der Waals forces and mass transfer.

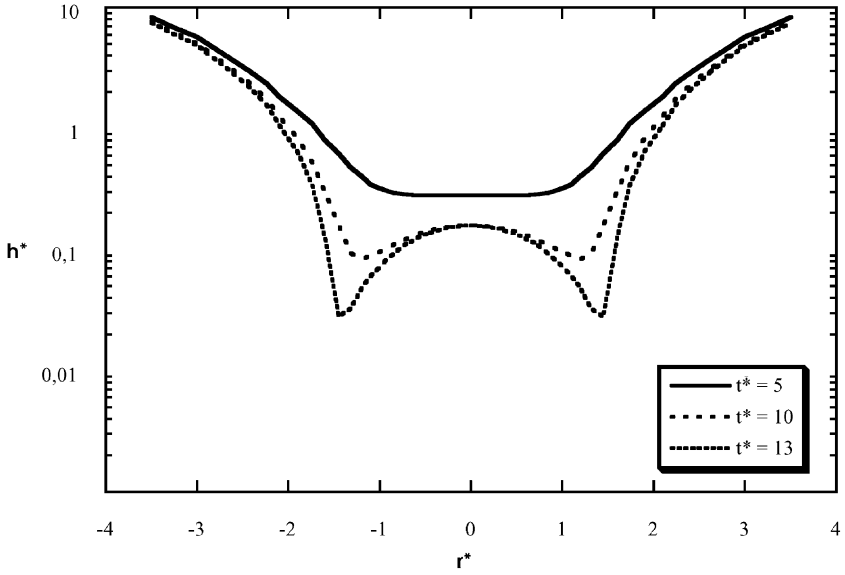

Fig. 3. Dimensionless film thickness, h^*, as a function of dimensionless radial position, r^*, and dimensionless time, t^*, in the presence of mass transfer for $Ma = -1$, $Pe = 250$, $Pe_d = 25\,000$ and $P = 1$ ($D \rightarrow C$).

3.2. Expression of the models I and II in transformed variables

Expressed in terms of transformed variables used in the numerical simulations (12) and (15) become

$$-\frac{k_1}{2h_{\min}^{*2}}\frac{\mathrm{d}h_{\min}^*}{\mathrm{d}t^*} = 1 - \frac{Ma}{(1+P)h_{\min}^*} = F_1 \qquad (12^*)$$

$$-\frac{k_1}{2h_{\min}^{*2}}\frac{\mathrm{d}h_{\min}^*}{\mathrm{d}t^*} = 1 - \frac{Ma\,Pe^{1/2}}{2k_2(1+P)t^{*1/2}} = F_2 \qquad (15^*)$$

where F_1 and F_2 denote the instantaneous drainage rate relative to that in the absence of mass transfer.

3.3. Drainage in the absence of mass transfer: the value of k_1

The next step is to obtain the value of k_1 from numerical results in the absence of mass transfer, for which (12*) and (15*) reduce to

$$-\frac{1}{h_{\min}^{*2}}\frac{\mathrm{d}h_{\min}^*}{\mathrm{d}t^*} = \frac{2}{k_1} \qquad (17)$$

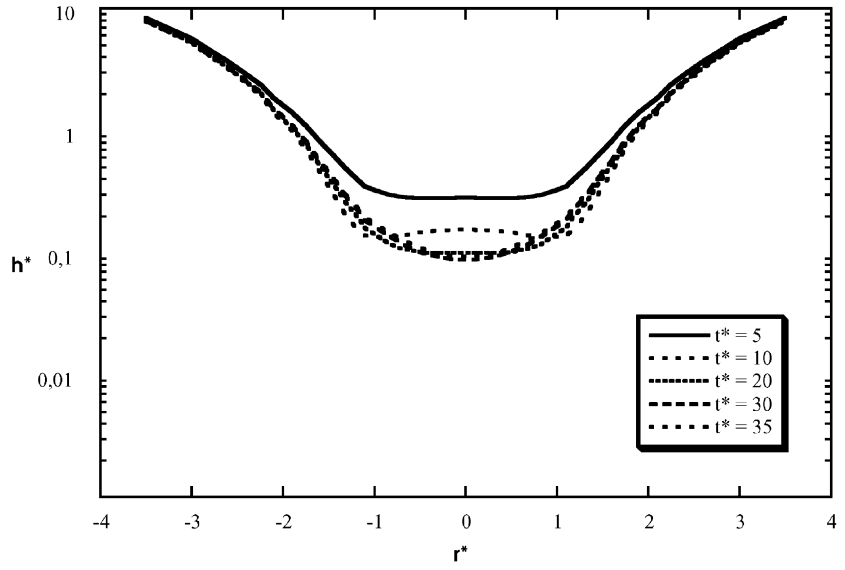

Fig. 4. Dimensionless film thickness, h^*, as a function of dimensionless radial position, r^*, and dimensionless time, t^*, in the presence of mass transfer for $Ma = 1$, $Pe = 250$, $Pe_d = 25\,000$ and $P = 1$ ($C \rightarrow D$).

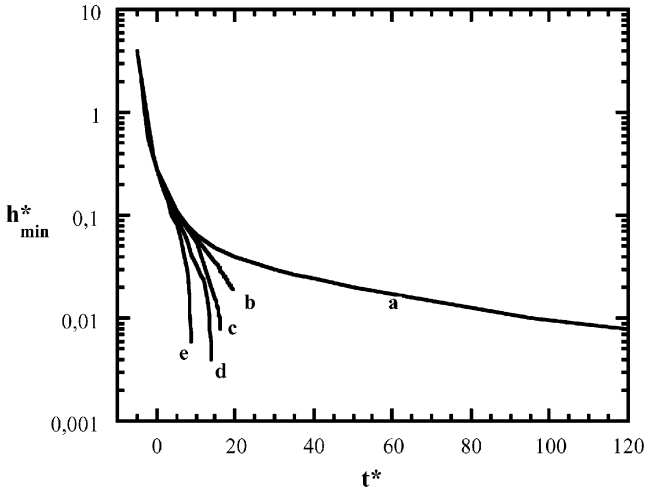

	a	b	c	d	e
Ma	0	-0.5	-0.5	-0.5	-1
Pe	-	250	250	250	250
Pe_d	-	$2.25\ 10^5$	$2.25\ 10^5$	$2.5\ 10^4$	$2.5\ 10^4$
P	-	1	3	1	3

Fig. 5. Dimensionless minimum film thickness, h^*_{min}, versus dimensionless time, t^*, in the presence of mass transfer, for different values of *Ma*, *Pe*, Pe_d and *P*, in the case of mass transfer occurring from dispersed to continuous phase.

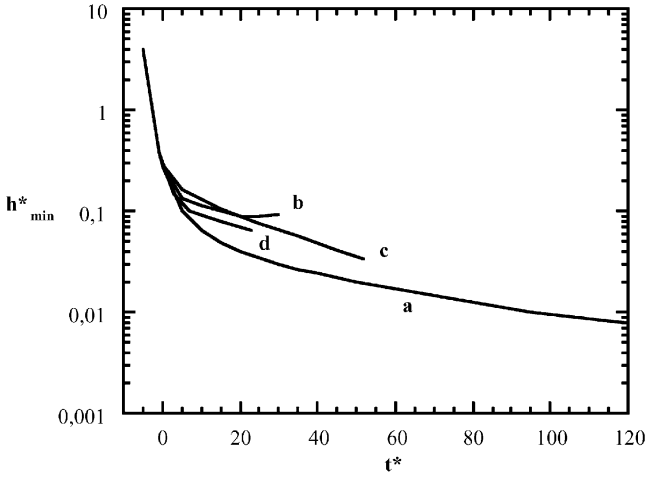

	a	b	c	d
Ma	0	1	1	0.5
Pe	-	16	250	250
Pe_d	-	4756	$2.5\ 10^4$	$2.5\ 10^4$
P	-	1	1	1

Fig. 6. Dimensionless minimum film thickness, h^*_{min}, versus dimensionless time, t^*, in the presence of mass transfer, for different values of *Ma*, *Pe*, Pe_d and *P*, in the case of mass transfer occurring from continuous to dispersed phase.

Table 1
Variation of h^*_{min} and related quantities during film drainage. The t^* origin has chosen to correspond with the onset of flattening around $h_{min} = 0.28$

t^*	h^*_{cen}	h^*_{min}	r^*_{min}	$-dh^*_{min}/dt^*$	$-(1/h^{*2}_{min})(dh^*_{min}/dt^*)$
−4	2.35	2.35	0	2.05	0.371
−3	1.051	1.051	0	0.7399	0.670
−2	0.5723	0.5723	0	0.2915	0.890
−1	0.3757	0.3757	0	0.1285	0.910
0	0.2830	0.2813	0.451	0.07289	0.921
10	0.1246	0.06587	1.187	0.005111	1.178
20	0.01012	0.03969	1.187	0.001415	0.898
30	0.08894	0.02974	1.187	0.0007075	0.800
40	0.08085	0.02421	1.187	0.0004512	0.770
50	0.07476	0.02033	1.187	0.0003343	0.809
60	0.06991	0.01734	1.187	0.0002674	0.889
70	0.06586	0.01492	1.187	0.0002192	0.985
80	0.06239	0.01293	1.187	0.0001818	1.087

The results (Table 1) indicate that $(1/h^{*2}_{min})(dh^*_{min}/dt^*)$ is indeed fairly constant, tough a slow oscillation is observable. This may be due to the fact that the value of h^*_{min}, from which the value of dh^*_{min}/dt^* were computed, are those in the grid point having the smallest h^*, which may or may not be close to the exact location of minimum h^*. Following flattening, the mean value of $(1/h^{*2}_{min})(dh^*_{min}/dt^*)$ is about 0.926, corresponding to $k_1 = 2.16$.

3.4. Drainage in the presence of mass transfer

3.4.1. Transfer from dispersed to continuous phase

Table 2a and b present the results for two values of *Ma* −0.5 and −1 for the above values of *Pe*, Pe_d and *P* (250, 2.5×10^4 and 1, respectively). F_{num} denotes the instantaneous value of dh^*_{min}/dt^*, relative to that in the absence of mass transfer (calculated from numerical simulations). $r^*_{h\,min}$ and r^*_{dcmin} denote the respective radii at which h^* exhibits a minimum and $\partial C_0/\partial r$ a maximum.

While the numerical values exhibit a certain oscillation, more pronounced for the larger *Ma*-value, it is clear that they correspond well with model I in the later stages of drainage. The poor initial correspondence may be ascribed to the fact that concentration boundary layers have barely met, so that the approximation of equilibration between film and drop is not yet applicable. This effect is weaker for smaller value of *Pe*, the initial thickness of the concentration boundary layers being (Appendix C):

$$\delta^* \sim \frac{1}{2}\left(\frac{\mu_d D}{R_{eq}\sigma (a')^5}\right)^{1/3} \sim \frac{1}{2Pe^{1/3}} \tag{18}$$

Table 2c–e provides additional data for different values of the parameters *Pe*, Pe_d and *P*. The results again provide evidence for the validity of model I if allowance for the numerical oscillations is made. In addition, Table 2e confirms that the correspondence with the model is observed earlier for smaller *Pe*-value.

Table 2
Comparison of the instantaneous accelerator factor, F_{num}, due to mass transfer from dispersed to continuous phase with the values F_1 and F_2 obtained from the approximate models I and II

h^*_{cen}	h^*_{min}	$-dh^*_{min}/dt^*$	r^*_{hmin}	r^*_{dcmax}	t^*	F_{num}	F_1	$F_2(k_2=1)$
(a) $Ma=-0.5$, $Pe=250$, $Pe_d=2.5\times10^4$, $P=1$								
2.35	2.35	2.05	0		−4			
1.05	1.05	0.730	0		−3			
0.570	0.570	0.290	0		−2			
0.375	0.375	0.129	0		−1			
0.282	0.280	0.0730	0.450		0	1.01	1.89	
0.231	0.218	0.0500	0.734	1.190	1	1.05	2.15	2.98
0.200	0.175	0.0400	0.950	1.320	2	1.41	2.43	2.40
0.180	0.142	0.0264	0.950	1.320	3	1.41	2.76	2.14
0.165	0.116	0.0220	1.065	1.450	4	1.77	3.16	1.99
0.155	0.0970	0.0200	1.190	1.450	5	2.30	3.58	1.89
0.148	0.0970	0.0148	1.190	1.450	6	1.70	3.58	1.81
0.144	0.067	0.0100	1.190	1.450	7	2.41	4.73	1.75
0.141	0.0540	0.0147	1.320	1.450	8	5.44	5.67	1.70
0.140	0.0410	0.0100	1.320	1.600	9	6.42	7.10	1.66
0.140	0.0330	0.0070	1.320	1.600	10	6.94	8.58	1.63
0.142	0.0266	0.0047	1.320	1.600	11	7.17	10.4	1.60
(b) $Ma=-1$, $Pe=250$, $Pe_d=2.5\times10^4$, $P=1$								
2.35	2.35	2.05	0		−4			
1.05	1.051	0.74	0		−3			
0.570	0.570	0.292	0		−2			
0.370	0.375	0.130	0		−1			
0.280	0.280	0.0730	0.450		0	1.01	2.79	
0.230	0.220	0.0510	0.730	1.190	1	1.14	3.27	4.95
0.190	0.170	0.0420	0.950	1.320	2	1.57	3.94	3.79
0.180	0.140	0.0350	1.00	1.450	3	1.93	4.57	3.28
0.170	0.100	0.0230	1.00	1.450	4	2.48	6.00	2.98
0.160	0.0830	0.0210	1.19	1.450	5	3.29	7.02	2.77
0.150	0.0630	0.0260	1.32	1.450	6	7.07	8.94	2.61
0.150	0.0420	0.0150	1.32	1.600	7	9.18	12.9	2.49
(c) $Ma=-1$, $Pe=250$, $Pe_d=2.25\times10^5$, $P=1$								
0.282	0.280	0.07289	0.451		0	1.01	1.89	
0.154	0.106	0.0150	1.06	1.32	5	1.44	3.36	1.89
0.131	0.0543	0.0063	1.19	1.45	10	2.31	5.60	1.63
0.136	0.0159	0.0064	1.32	1.45	15	27.3	16.7	1.51
(d) $Ma=-1$, $Pe=250$, $Pe_d=2.25\times10^5$, $P=3$								
0.282	0.280	0.0731	0.451		0	1.01	1.45	
0.154	0.107	0.0148	1.06	1.32	5	1.40	2.17	1.44
0.127	0.0586	0.0058	1.19	1.45	10	1.82	3.13	1.31
0.121	0.0351	0.0050	1.32	1.45	15	4.38	4.56	1.26
0.125	0.0198	0.0028	1.32	1.45	19	7.71	7.48	1.23
(e) $Ma=-1$, $Pe=16$ and $Pe_d=4756$, $P=1$								
0.276	0.273	0.0838	0.541		0	1.21	2.83	
0.221	0.201	0.0630	0.839	1.32	1	1.68	3.49	4.95
0.188	0.147	0.0512	1.06	1.45	2	2.56	4.40	3.79
0.169	0.106	0.0353	1.19	1.59	3	3.39	5.72	3.28
0.157	0.0754	0.0274	1.32	1.59	4	5.20	7.63	2.98
0.151	0.0527	0.0336	1.45	1.74	5	13.1	10.5	2.77
0.149	0.0298	0.0136	1.45	1.74	6	16.5	17.8	2.61

3.4.2. Transfer from continuous to dispersed phase

Table 3a presents the results for the set parameters: $Ma=1$, $Pe=16$, $Pe_d=4756$ and $P=1$. The later stages of drainage correspond reasonably well with model II, taking $k_2=1$. Based on the few data points in this region, it is not possible to refine the value of k_2.

Results for $Ma=1$, $Pe=250$, $Pe_d=2.5\times10^4$ and $P=1$ are presented in Table 3b. According to model II, F_2 is negative (i.e. Marangoni effects cause h^*_{min} to increase) if $0<t^*<Pe[Ma/2k_2(1+P)]^2$. In the case considered in Table 3a, range of times for which F_2 is negative is small: $0<t^*<1$, taking $k_2=1$. For the case treated in Table 3b,

Table 3
Film drainage for mass transfer from continuous to dispersed phase

h^*_{cen}	h^*_{min}	$-dh^*_{min}/dt^*$	r^*_{hmin}	r^*_{dcmax}	t^*	F_{num}	F_1	$F_2(k_2=1)$
(a) $Ma=+1, Pe=16, Pe_d=4756, P=1$								
0.289	0.288	0.0641	0.366	1.32	0	0.835	−0.74	
0.173	0.165	0.00907	0.734	1.450	5	0.360	−2.03	0.553
0.108	0.106	0.00400	0.451	1.450	15	0.384	−3.7	0.742
0.0781	0.0761	0.00231	0.451	1.59	25	0.431	−5.6	0.8
0.0604	0.0563	0.00167	0.541	1.59	35	0.569	−7.9	0.831
0.0487	0.0415	0.00122	0.635	3.75	45	0.765	−11	0.851
0.0429	0.0334	0.00106	0.734	4.01	52	1.03	−14	0.861
(b) $Ma=+1, Pe=250, Pe_d=2.5\times10^4, P=1$								
0.282	0.280	0.0730	0.450		0	1.01	−0.779	
0.154	0.133	0.0074	0.949	1.31	5	0.337	−2.76	−0.766
0.120	0.114	0.0031	0.630	1.31	10	0.258	−3.39	−0.249
0.101	0.101	0.0027	0.21	1.31	15	0.259	−3.95	−0.020
0.0900	0.0900	0.00124	0	1.31	20	0.165	−4.56	0.117
0.0880	0.0880	−0.000	0	1.31	25	−0.00	−4.68	0.210
0.0930	0.0930	−0.000	0	1.31	30	−0.00	−4.10	0.278

however, *Pe* is much larger and the range of negative F_2-value becomes $0 < t^* < 15.6$. Once more neglecting the initial period of drainage, the numerical results do qualitatively reflect this expectation, F_{num} being falling below zero in the final stage of the computations. The fact that F_{num} does not become strongly negative suggests that positive values would soon reappear were the computation further pursued. While a better match between model and numerical results could be obtained by reducing the value of k_2 (thereby increasing the t^* range for which the model predicts negative F_2-value), this is probably not justified since the concentration boundary layer thickness is probably of the same order as the film thickness throughout the computation in view of the large value of *Pe* (see Eq. (18)) combined with the large values of h^*_{min}.

3.4.3. Range of applicability of models I and II

While the numerical results provide satisfactory support for model I in the cases of transfer from dispersed to continuous phase, a problem remains: model II contains no specific assumptions about the direction of transfer and might be expected to apply in all cases. The explanation is provided by the value of r^*_{hmin} and r^*_{dcmax}, illustrated vividly by the results in Table 2e, as the region of maximum interfacial concentration gradient move radially outwards the location of minimum thickness follows. The associated physical picture is as follows. As soon as the location of maximum Marangoni forces moves beyond the edge of the film, thinning accelerates in this region, which is promptly incorporated in the film, so that the region of the maximum Marangoni force permanently coincides with that of minimum film thickness as assumed in model I. The fact that r^*_{dcmax} is slightly larger than r^*_{hmin} is explained by the fact that the Marangoni force per unit volume of the film is given by $(2/h)(\partial\sigma/\partial r)$, so that its maximum value is developed at smaller h^*-values (and hence r^*-values) than that of $(\partial\sigma/\partial r)$ (or equivalently, $(\partial C_0/\partial r)$).

It is evident that for sufficiently small values of the Marangoni parameter *Ma*, or sufficiently large value of the parameter determining boundary layer growth rates, *Pe*, the zone of minimum film thickness will no longer be able to keep up with the radial expansion of the zone of maximum interfacial concentration gradient and drainage will be described by model II rather than model I. No information on the location of this transition in parameter-space is provided by the available numerical results. It is conceivable that when the transition results from a very small *Ma*-value, the associated Marangoni effects are so weak as to be negligible according to either model. Likewise, very small values of *Pe* might arise as a result either of small a'-values (gentle collisions) or of large μ_d/μ-values (large $\mu_d D$). Predicted coalescence probabilities would then in all likelihood remain closer to 1 or 0, respectively, whichever model is applied. It is thus possible, though undemonstrated, that model I suffices for all practical purposes whenever transfer is from dispersed to continuous phase and this is assumed to be the case in what follows. Numerical exploration of the transition conditions is, however, desirable.

In the case of mass transfer from continuous to dispersed phase, thinning is suppressed by Marangoni forces and there is no driving force for the region of minimum film thickness to follow that of maximum interfacial concentration gradient. Model II should therefore describe (the late stages of) drainage in all cases.

4. The critical film rupture

4.1. Model I

Applying the same approach as in the absence of mass transfer [8], the critical film-rupture thickness in the case of Marangoni accelerated film drainage should be given by:

$$F_w \sim F_p + F_\sigma \tag{19}$$

where F_w denotes the radial force per unit volume of film due to the reduction of the film tension associated with van der Walls forces:

$$F_w \sim \frac{1}{h}\frac{\Delta\Sigma}{a} \sim \frac{A}{4\pi a h^3} \tag{20}$$

where Σ is the film tension ($= 2\sigma - A/4\pi h^2$), A the Hamaker constant. Substituting (2), (10) and (20) into (19), an implicit relation for the critical film-rupture thickness, h_c, is obtained:

$$\left(\frac{h_{c,0}}{h_c}\right)^3 = 1 + \frac{h_M}{h_c} \tag{21}$$

where $h_{c,0}$ denotes the value of h_c in the absence of mass transfer

$$h_c \sim \left(\frac{AR_{eq}}{8\pi\sigma}\right)^{1/3} \tag{22}$$

This approximate analytical expression were compared by Saboni et al. [7] with complete numerical simulations in the presence of van der Waals forces and in the absence of mass transfer. It was found that expression (22) provide a good first approximation for the critical film-rupture thickness.

In the case of Marangoni domination in the final stages of drainage ($h_c \ll h_m$), (21) reduces to

$$h_c = \left(\frac{h_{c,0}^3}{h_M}\right)^{1/2} \sim \left(\frac{A}{8\pi\Delta\sigma}\right)^{1/2} \tag{23}$$

4.2. Model II

An approximate expression for the effective critical film-rupture thickness is provided by the expression in the absence of Marangoni effects

$$h_c \sim \left(\frac{k_3 AR_{eq}}{8\pi\sigma}\right)^{1/3} \quad \text{where } k_3 \sim 1 \tag{24}$$

in which σ is replaced by the effective value obtained from (15)

$$\sigma_{eff} \sim \sigma\left(1 + \frac{R_{eq}\Delta\sigma}{2k_2\sigma(Dt)^{1/2}}\right) \tag{25}$$

combination of (24) and (25) now yields

$$\frac{k_3 AR_{eq}}{8\pi\sigma h_c^3} = 1 + \frac{R_{eq}\Delta\sigma}{2k_2\sigma(Dt)^{1/2}} \tag{26}$$

Expressed in terms of transformed variables (24) become

$$\frac{k_3 A^*}{2h_c^{*3}} = 1 - \frac{Ma\,Pe^{1/2}}{2k_2(1+P)(t_c^*)^{1/2}} \tag{26*}$$

where $A^* = A/4\pi\sigma R_{eq}^2 (a')^6$

5. Drainage time

5.1. Model I

Eq. (12) may be expressed as

$$-T\frac{h_M}{h^2}\frac{dh}{dt} = 1 + \frac{h_M}{h} \tag{27}$$

where $T = \mu_d a/2\Delta\sigma$ In the constant case (a constant) and for h_M, (27) integrates to give

$$t = T\ln\left(\frac{1 + (h_M/h)}{1 + (h_M/h_{flat})}\right) \tag{28}$$

where t denotes the time to drain from the onset of flattening to the thickness h.

The time, t_c, to drain from h_{flat} to h_c follows from (21) and (27). To obtain an indication of the influence of Marangoni forces, the drainage time, $t_{c,0}$, is compared with t_c for the case $h_c \ll h_M \ll h_{flat}$, in which an explicit expression is provided by (23) and (27)

$$t_c = \frac{3}{2}T\ln\left(\frac{h_M}{h_{c,0}}\right) \tag{29}$$

The drainage time in the absence of mass transfer is obtained from (23) and (27) in the limit of $h_M \to 0$

$$t_{c,0} = T\frac{h_M}{h_{c,0}} \tag{30}$$

Accordingly

$$\frac{t_c}{t_{c,0}} = \frac{3}{2}\frac{h_{c,0}}{h_M}\ln\left(\frac{h_M}{h_{c,0}}\right) \tag{31}$$

This expression indicate earlier rupture for $D \to C$ mass transfer. For instance, if $h_M/h_{c,0}$ is equal to $10(t_c/t_{c,0})$ is equal to 0.35.

5.2. Model II

The value of the time, t_c, to drain to rupture in the presence of mass transfer follows from (15*) and (26*). In the limit of no mass transfer the second term in the RHS of (15*) and (26*) disappears

$$\frac{k_1}{2h_{c,0}^*} = t_{c,0}^* \tag{15_0*}$$

$$\frac{k_3 A^*}{2h_{c,0}^{*3}} = 1 \tag{26_0*}$$

Dividing (15*) by (15_0*) and (26*) by (26_0*) now yields:

$$\frac{1}{fH_c} = 1 - \frac{Z}{f^{1/2}} \tag{32}$$

$$\frac{1}{H_c^3} = 1 - \frac{Z}{2f^{1/2}} \tag{33}$$

with

$$H_c = \frac{h_c}{h_{c,0}} \tag{34}$$

and

$$Z = \frac{Ma\,Pe^{1/2}}{2k_2(1+P)(t^*_{c,0})^{1/2}} \tag{35}$$

where $t_{c,0}$ follows from (15_0*) and (26_0*), and $f = t_c/t_{c,0}$.

This expression indicates later rupture for $C \rightarrow D$ mass transfer. For a given value of the parameter Z, (32) and (33) are readily solved iteratively for f (and H_c). For example, taking $H_c = 1$ as a first approximation, (32) provides a quadratic equation for $f^{1/2}$ and (33) provides a better approximation to H_c, etc. For instance, taking $Z = 0.5$, the calculations give $f = 1.55$ and $H_c = 1.08$, while for $Z = 10$ the calculations give $f = 102$ and $H_c = 1.26$.

5.3. Coalescence probability

In the presence of mass transfer, the expression for the coalescence probability [8,10,11]

$$P = \exp\left(-\frac{t_c}{t_i}\right) \tag{36}$$

becomes

$$P = \exp\left(-\frac{f\,t_{c,0}}{t_i}\right) = (P_0)^f \tag{37}$$

where P_0 is the coalescence probability in the absence of mass transfer. For a given P_0 [8], expression (37) can be used when mass transfer is from dispersed to continuous phase and also if mass transfer is from continuous to dispersed phase, making use of appropriate expressions for the acceleration/deceleration factor f.

6. Conclusion

Two simple analytical models for predicting the influence of interphase mass transfer on coalescence in liquid–liquid dispersions were developed. The models describe drainage and rupture of partially mobile films during coalescence in the presence of mass transfer. The results obtained from the analytical models were compared with a more sophisticated model (numerical simulation results); within a certain limit of accuracy, the two sets are in agreement. In the case of Marangoni-accelerated drainage, corresponding typically to mass transfer from the dispersed to the continuous phase ($D \rightarrow C$), expressions have been derived for the time required for drainage to rupture. Even relatively small concentration differences are predicted to dramatically accelerate drainage. In the reverse case of Marangoni-retarded drainage (mass transfer from continuous to dispersed ($C \rightarrow D$)) the time required for drainage to rupture is enhanced. At large times, the model II predicts an asymptotic return to the drainage rate in the absence of mass transfer. The range of applicability of each model is considered and expressions for the film rupture required for the coalescence probability are developed which may be used in two phase flow simulations.

Appendix A

A.1. Interface concentrations

The first interface condition assumes quasi-equilibrium solute partition

$$\frac{dC_d}{dC} = K = \text{constant} \tag{A.1a}$$

or

$$C_d = K(C + c) \quad (c \text{ is a constant}) \tag{A.1b}$$

A.2. Influence of the velocity induced by mass transfer on the mass flux trough the interface

The barycentric mixture velocity, $\mathbf{u}$, is defined as

$$\rho u = \rho_A \mathbf{u}_A + \rho_B \mathbf{u}_B \tag{A.2}$$

where A refers to solute and B to solvent (be this the continuous or the dispersed phase). With respect a reference frame translating with a material point on the interface, $\mathbf{u}[0, 0, u_z]$, where the z-direction is that of the outward normal. At the interface $(u_z)_B = 0$ and (A.2) yields

$$u_z = \frac{\rho_A}{\rho}(u_z)_A = C_0(u_z)_A, \quad z = 0 \tag{A.3}$$

The difference between $(u_z)_B$ and $(u_z)_A$ is given by Fick's law

$$m = \rho_A[(u_z)_A - u_z] = -\rho D\frac{\partial C}{\partial z} \quad \text{or}$$

$$C[(u_z)_A - u_z] = -D\frac{\partial C}{\partial z} \tag{A.4}$$

Elimination of $(u_z)_A$ from (A.3) and (A.4) now leads to

$$(u_z)_0 = -\frac{D}{1 - C_0}\frac{\partial C}{\partial z} \tag{A.5}$$

which, with the help of (A.3) leads to

$$\rho_d D'_d \frac{\partial C_d}{\partial z} = \rho D' \frac{\partial C}{\partial z} \tag{A.6a}$$

where

$$D' = \frac{D}{1 - C_0} \tag{A.6b}$$

and

$$D'_d = \frac{D_d}{1 - K(C_0 + c)} \tag{A.6c}$$

Appendix B

B.1. Diffusion at a dilating interface

As preliminary, consider a semi-infinite region of liquid with constant solute concentration, C_0, at its plane boundary and constant concentration, C_∞ at $z = \infty$, where z denotes distance along the normal to the boundary. If the only source of flow is that induced by a uniform dilation of the boundary, which is transmitted by viscous action to the adjoining liquid.

$$\frac{1}{A}\frac{\mathrm{D}A}{\mathrm{D}t} = \frac{1}{T} \tag{B.1}$$

where A is area of material element of the interface. Then the z-component of the velocity follows from continuity

$$\frac{1}{A}\frac{\mathrm{d}A}{\mathrm{d}t} = \frac{\partial u_x}{\partial x} + \frac{\partial u_y}{\partial y} = -\frac{\partial u_z}{\partial z} \tag{B.2a}$$

$$u_z = -\frac{z}{T} \tag{B.2b}$$

Choosing the origin in a given material point on the boundary, the diffusion equation is

$$\frac{\partial C}{\partial t} + u\nabla C = D\nabla^2 C \tag{B.3}$$

at any point (0, 0, z) becomes

$$\frac{\partial C}{\partial t} - \frac{z}{T}\frac{\partial C}{\partial z} = \frac{\partial^2 C}{\partial z^2} \tag{B.4}$$

In the special case $T = \infty$ (non-dilating boundary), (B.4) can be integrated analytically

$$\frac{C - C_0}{C_0 - C_\infty} = 1 - \mathrm{erf}\left(\frac{z}{2\sqrt{\mathrm{D}t}}\right) \tag{B.5}$$

For a steady dilation (T = constant, $\partial C/\partial t = 0$), (B.4) yields

$$\frac{C - C_0}{C_0 - C_\infty} = 1 - \mathrm{erf}\left(\frac{\mathrm{z}}{\sqrt{2\mathrm{DT}}}\right) \tag{B.6}$$

The preceding considerations can be extended to a steadily dilating interface between semi-infinite regions of immiscible liquids. The concentration distributions in each phase will again be given by (B.6), the value C_0 and $C_{\mathrm{d},0}$ being determined by the interface conditions (A.1) and (A.6). Making use of (B.6), (A.6a) becomes

$$\rho_\mathrm{d} D'_\mathrm{d}(C_{\mathrm{d},0} - C_{\mathrm{d},\infty}) = \rho D'(C_0 - C_\infty) \tag{B.7}$$

which together with (A.1) yields

$$C_0 + c = \frac{C_\infty + c + P(C_{\mathrm{d},\infty})/K}{1 + P} \tag{B.8}$$

With the transformed partition parameter given by:

$$P = K\frac{\rho_\mathrm{d} D'_\mathrm{d}\sqrt{D}}{\rho D'\sqrt{D_\mathrm{d}}} \tag{B.9}$$

Appendix C

C.1. Concentration boundary layer thickness in the region outside the film

Once the separation of two drops, h, becomes less than 2δ, the boundary condition, C = constant = C_∞ at $z = \infty$, ceases to be a good approximation and ($C_{\mathrm{d},0}$) rises/falls towards ($C_{\mathrm{d},\infty}$), while the interfacial concentration outside the film is still given by (B.8). The onset of Marangoni effects, driven by the resulting variation of interfacial tension, thus corresponds to

$$h_\delta \sim 2\delta \tag{C.1}$$

The value of δ: Depending on whether h_δ is smaller or larger than h_flat (the film thickness at which the drops become flattened), the value of $-\mathrm{d}h/\mathrm{d}t$ can either be approximated as constant, corresponding to the approach velocity of centers, or decreasing as $h \sim 2$, corresponding to the drainage law for partially mobile, flat film [8]. In the former case, $-h^{-1}(\mathrm{d}h/\mathrm{d}t)$ increases as h^{-1}, in the latter it decreases as h^{+1}.

At the transition point $h_\delta \sim h_\mathrm{flat}$,

$$-\frac{1}{h}\frac{\mathrm{d}h}{\mathrm{d}t} = \text{constant} \tag{C.2}$$

Further from (B.2a,b)

$$\frac{1}{T} = -\frac{\Delta u_z}{\Delta_z} = -\frac{1}{h}\frac{\mathrm{d}h}{\mathrm{d}t}$$

an application of the analytical solution for constant T then yields

$$\delta = \sqrt{\frac{\pi D}{2}\frac{-h}{\mathrm{d}h/\mathrm{d}t}} \sim \sqrt{\frac{-Dh}{\mathrm{d}h/\mathrm{d}t}} \tag{C.3}$$

For $h_\delta > h_\mathrm{flat}$, δ decreases with time and its value will therefore lag somewhat behind that given by (C.3). Conversely, for $h_\delta < h_\mathrm{flat}$, δ will be somewhat smaller than the value given by (C.3). In both cases, however, (C.3) should be valid as an order of magnitude estimate.

Up to the point at which the film thickness h_δ is attained, $\mathrm{d}h/\mathrm{d}t$ will be approximated by the drainage law for drops of constant interfacial tension. For cases in which the drops are already flattened ($h_\mathrm{flat} > h_\delta$), this law is roughly [8]

$$\frac{\mathrm{d}h}{\mathrm{d}t} \sim -\frac{2(2\pi\sigma/R_\mathrm{eq})^{3/2}}{\pi\mu_\mathrm{d}F^{1/2}}h^2 \tag{C.4a}$$

or

$$\frac{\mathrm{d}h}{\mathrm{d}t} \sim -\frac{4\sigma}{\mu_\mathrm{d}R_\mathrm{eq}a}h^2 \tag{C.4b}$$

where a is a measure of the radius of the film, $F = \pi a 2\sigma/R_\mathrm{eq}$, where F is the drop interaction force. Combination of (C.3) and (C.4) yields

$$\left(\frac{2\delta}{h}\right)^2 \sim \frac{\mu_\mathrm{d}DaR_\mathrm{eq}}{\sigma h^3} \tag{C.5}$$

The value of h_δ:

$$h_\delta \sim 2\delta \sim \left(\frac{\mu_d Da R_{eq}}{\sigma}\right)^{1/3} \tag{C.6}$$

Expressed in terms of the transformed variables h_δ and δ become

$$\delta^* \sim \frac{1}{2}\left(\frac{\mu_d D}{R_{eq}\sigma (a')^5}\right)^{1/3} \sim \frac{1}{2Pe^{1/3}} \tag{C.7}$$

$$h^* \sim \left(\frac{\mu_d D}{R_{eq}\sigma (a')^5}\right)^{1/3} \sim \frac{1}{Pe^{1/3}} \tag{C.8}$$

Appendix D

D.1. Concentration boundary layer thickness in the region outside the film

The concentration boundary layer thickness, δ, in the region outside the film depends on the dilation history of the interface, which in turn depends on the Dh/Dt, h being linked to the interfacial area of material element, S, via constancy of the element's volume, hS.

Dh/Dt is given by

$$\frac{Dh}{Dt} = \frac{\partial h}{\partial t} + u\frac{\partial h}{\partial r} \tag{D.1}$$

The film velocity, $u(r)$, in the outer region fellows from continuity if $h(r)$ is approximated as corresponding to a film of negligible thickness, beyond which drops are undeformed

$$h = 0, \quad r \le a \tag{D.2}$$

$$h = \frac{r^2 - a^2}{R_{eq}}, \quad r \ge a \tag{D.3}$$

$$2\pi r u h = \pi (r^2 - a^2) V, \quad r \ge a \tag{D.4}$$

where V denotes the instantaneous approach velocity of the undeformed portions of the drops

$$V = -\frac{\partial h}{\partial t} \tag{D.5}$$

Combination of (D.1)–(D.5) now yields

$$\frac{Dh}{Dt} = V\left(-1 + \frac{r^2 - a^2}{2rh}2\frac{r}{R_{eq}}\right) \tag{D.6}$$

Indicating the absence of dilation (h and hence S constant)

If the continuous phase-concentration boundary layer thickness, δ, is defined as

$$\left(\frac{\partial C}{\partial z}\right)_{z=0} = \frac{C_\infty - C_0}{\delta} \tag{D.7}$$

then its value in the case of non-dilating interface is obtained by differencing (B.5)

$$\delta \sim \sqrt{(Dt)} \tag{D.8}$$

and the film thickness, h_δ, in the region where the concentration boundary meet is thus given by

$$h_\delta \sim 2\sqrt{(Dt)} \tag{D.9}$$

(D.8) ignores the fact that at the onset of flattening ($t = 0$), δ, is already non-zero. The associated error is small, however, as the overall drainage time is dominated by the final stages of drainage for which (D.8) is acceptable.

References

[1] F. Kleczek, V. Cauwenberg, P. Van Rompay, Chem. Eng. Technol. 12 (1989) 395.
[2] C. Gourdon, G. Casamatta, Chem. Eng. Sci. 46 (1991) 2799.
[3] A. Saboni, C. Gourdon, A.K. Chesters, Chem. Eng. Sci. 54 (1999) 461.
[4] S.G. Yiantsios, R.H. Davis, J. Fluid Mech. 217 (1990) 547.
[5] S. Abid, A.K. Chesters, Int. J. Multiphase Flow. 20 (1994) 613.
[6] S.G. Yiantsios, R.H. Davis, J. Colloid Interf. Sci. 144 (1991) 412.
[7] A. Saboni, C. Gourdon, A.K. Chesters, J. Colloid Interf. Sci. 173 (1995) 27.
[8] A.K. Chesters, Trans. I Chem. E 69 (Part A) (1991) 239.
[9] M.J. Kourio, Ph.D. Thesis, Institut National Polytechnique de Toulouse, 1989.
[10] M.J. Kourio, C. Gourdon, G. Casamatta, Chem. Eng. Technol. 17 (1994) 249.
[11] S.I. Ross, F.H. Verhoff, R.I. Curl, Ind. Eng. Chem. Fundl. 16 (1977) 371.